



**Acoustics'08
Paris**
June 29-July 4, 2008

www.acoustics08-paris.org

Multi-input multi-output OFDM for shallow-water UWA communications

Yunus Emre^a, Vinod Kandasamy^a, Tolga Duman^a, Paul Hursky^b and
Subhadeep Roy^c

^aArizona State University, Dept. of Electrical Engineering, Tempe, AZ 85287-5706, USA

^bHLS Research, Inc., 3366 N. Torrey Pines Ct., Ste. 310, La Jolla, CA 92037, USA

^cQualcomm Flarion Technologies, Bridgewater, NJ 08807, USA

duman@asu.edu

We investigate the performance of turbo coded multiple-input multiple-output (MIMO) orthogonal frequency division multiplexing (OFDM) systems with layered space time (LST) architectures for underwater acoustic (UWA) channels. We present results obtained by processing data from the AUVfest07 experiment performed in June 2007. We review the necessary components of a MIMO-OFDM communication system, including time/frequency synchronization and channel estimation, and we summarize modifications needed to make the system suitable for UWA channels. We find that the results of the AUVfest 2007 experiment are very promising in terms of achieved data rates and error rate performance of the system. We also present results for differential MIMO-OFDM modulation techniques, that potentially would provide additional robustness in more difficult channels.

1 Introduction

Underwater acoustic channels are characterized by severe bandwidth limitations, long intersymbol interference (ISI) spans and high Doppler spreads leading to significant challenges for reliable communications. Over the past several decades, many different transmission schemes have been proposed for these systems to improve transmission rates and to reduce error rates. For instance, a useful approach is to employ adaptive decision feedback equalization techniques with embedded digital phase lock loops to track the channel variations and Doppler shifts [1]. This technique and its extensions are very powerful. However, the required complexity for decoding/equalization presents challenges to realizing a practical implementation.

Orthogonal frequency division multiplexing may be a good alternative that both remedies the problem of ISI and provides low complexity solutions that can be implemented in practical systems. OFDM is a multicarrier transmission scheme widely used in wireless radio communications. It has also been proposed for use in shallow water UWA communications [2–6]. The main idea is to split the available frequency band into many narrow subbands, and transmit different symbols simultaneously in each subband. The carrier spacing is selected so that the carriers are orthogonal, which coincides with the spacing of Fast Fourier Transform (FFT) bins, enabling both the transmit and receive processing chains to exploit the efficiency of FFTs in their implementations. Since each of the subcarriers sees an effectively flat channel, the problem of ISI is mitigated.

Time variations of the UWA channel may be detrimental in an OFDM system since the orthogonality of the different subcarriers may be compromised. Effects of Doppler shifts can be overcome using resampling of the received signal as employed in [6], and if the Doppler spreads are not very significant (i.e. the remaining time variations do not cause important channel variations over one OFDM symbol), this scheme can be very effective.

Channel coding schemes can also be used in OFDM systems. In this case, since the codewords are transmitted on multiple subcarriers, the resulting redundancy across frequencies provides frequency diversity.

A number of results have been published about OFDM systems for UWA communications. For example, data rates between 5.3 kbps and 12 kbps over 24 kHz bandwidth and 350 m range for very shallow water have been reported in [5].

For fading channels, it has been found that MIMO systems offer significantly increased channel capacity, leading to much higher transmission rates [7]. Alternatively,

MIMO systems can also provide spatial diversity when space-time coding schemes are employed [8]. As reported in [9], various MIMO communication techniques (offering varying combinations of diversity gain and spatial multiplexing) have been shown to be very effective for UWA communication channels, when combined with MIMO decision feedback equalization (DFE) and digital phase locked loops (PLLs). As a specific example, a transmission rate of 48 kbps with a 4×4 MIMO system with turbo coding has been demonstrated using at-sea test data [9].

More recently, some results combining MIMO techniques with OFDM have also been reported [6, 10]. These papers describe phase-coherent modulation of each subcarrier, with zero-padding as an alternative to the more typical cyclic prefix (used to preserve the orthogonality of the carriers in the presence of multipath). Probe signals and null subcarriers are typically used for timing and frequency synchronization. Rate $\frac{1}{2}$ low-density parity-check (LDPC) coding and QPSK modulation are used with 1024 subcarriers in [10], which reports data rates of 12.18 kbps over a bandwidth of 12 kHz for ranges of 500 m and 1500 m. In [6], rate $\frac{2}{3}$ convolutional coding and QPSK modulation are used with varying numbers of subcarriers (512, 1024 and 2048) to achieve a 9.7 kbps data rate over a 12 kHz bandwidth.

Our main objective in this paper is to provide a treatment of MIMO-OFDM for UWA channels, and present processing results from the AUVfest 2007 experiment. We have tested both fully coherent and differential MIMO modulation schemes, in both cases using turbo codes for channel coding. Note, however, that Doppler shifts were low, and significant time variations were not encountered in this channel, so we have not addressed their impact upon MIMO-OFDM performance.

The paper is organized as follows. Transmission schemes are presented in Section 2. Receiver structures are described in Section 3. Using these transmissions and receiver structures, Section 4 presents results of processing data from the AUVfest 2007 experiment. Conclusions are presented in Section 5.

2 OFDM Transmission Schemes

In our OFDM scheme, the information bits are encoded using a turbo code. The coded bits are interleaved and mapped to a phase-shift keying (PSK) constellation. The resulting complex symbols are passed through a serial-to-parallel converter and an inverse FFT, a cyclic prefix is added, and the resulting baseband waveform is bandshifted up to the carrier for transmission. For spatially multiplexed MIMO systems, the general structure is replicated at each transmit element and multiple in-

dependent data streams are transmitted simultaneously in the same frequency band.

2.1 Coherent MIMO-OFDM

In coherent MIMO-OFDM, a subset of the subcarriers is reserved as pilot tones, to be used for channel estimation. Optimal placement of pilot symbols depends on the frequency characteristics of the channel. However, to reduce complexity, they are usually periodically spaced. For an m transmit element system, the pilot symbols form an $m \times m$ non-singular matrix. Note that one can allocate a larger number of consecutive subcarriers as pilots, however, m is the minimum number needed to estimate all m channel coefficients corresponding to all the transmit elements. For instance, in a two transmit element system, the pilot signals are of the form $\mathbf{X}_k = \begin{pmatrix} X_k^1 & X_k^2 \\ X_{k+1}^1 & X_{k+1}^2 \end{pmatrix}$ where X_k^i is the pilot signal transmitted at the k^{th} subcarrier for the i^{th} transmit element. A simple example is $\mathbf{X}_k = \begin{pmatrix} 1 & -1 \\ 1 & 1 \end{pmatrix}$. If the number of transmit elements is larger, for example, Hadamard matrices can be used.

2.2 Differential Schemes

In addition to the coherent transmission schemes described in Section 2.1, we also consider differential schemes to eliminate the need for channel estimation. With a single transmit element, the transmitted symbols are picked from a PSK constellation, i.e., $\{u_k = e^{j\phi_k}\}$, $k \in \{0, \dots, N-1\}$, and the information is embedded in the phase differences of the symbols transmitted using consecutive subcarriers. For a differential M-PSK scheme, the phases used are $\phi_k = \frac{2\pi m_k}{M}$, with $m_k \in \{0, \dots, M-1\}$. The sequence of N symbols, $\{X_k\}$, is transmitted using the N subcarriers. We emphasize that the differential encoding is done across different subcarriers (in frequency), not in time.

There are different classes of codes that can be used for differential MIMO-OFDM. In this paper, we focus on a particular differential space-time modulation scheme with implicit channel coding as described in [14]. The difference here is that the coding is done across frequency, and the scheme is a differential space-frequency code that exploits the fact that the adjacent subcarriers normally undergo similar channel fades.

In [14], group codes are used. A group \mathcal{G} consists of a set of code matrices. Depending on the input sequence, a code matrix “ \mathbf{G} ” is chosen from the group and transmitted over multiple elements (and multiple subcarriers). As an example, let us consider the group of matrices with QPSK symbols from [14],

$$\mathcal{G} = \left\{ \mp \begin{pmatrix} 1 & 0 \\ 0 & 1 \end{pmatrix}, \mp \begin{pmatrix} j & 0 \\ 0 & -j \end{pmatrix}, \mp \begin{pmatrix} 0 & 1 \\ -1 & 0 \end{pmatrix}, \mp \begin{pmatrix} 0 & j \\ j & 0 \end{pmatrix} \right\}.$$

For this code, since there are eight different matrices that determine what is transmitted for two subcarriers, three incoming bits are used together with what is transmitted in the previous set of subcarriers, resulting in a spectral efficiency of 1.5 bits/sec/Hz. The transmission is initialized by $\mathbf{X}_0 = \mathbf{D} = \begin{pmatrix} 1 & -1 \\ 1 & 1 \end{pmatrix}$. Thereafter, the k^{th} transmission block is given by $\mathbf{X}_k = \mathbf{X}_{k-1} \mathbf{G}_k$. For the general case, the dimensions of \mathbf{X}_k is $m \times t$,

where t is the consecutive number of subcarriers encoded together.

2.3 Turbo Coding with MIMO-OFDM

Turbo codes can be effective in reducing error rates in MIMO-OFDM systems. The idea is to introduce redundancy with an outer code before modulating the transmitted bits, and to exploit this redundancy at the receiver. Since the different bits comprising the code-words are transmitted over different frequency bands, the channel coding in this case adds redundancy across frequencies, and may provide additional frequency diversity. We chose to use the standard turbo coding configuration of parallel concatenated recursive convolutional codes separated by an interleaver. At the receiver, the turbo decoder is fed with soft decisions about each coded bit, which are decoded by an iterative algorithm using maximum a-posteriori (MAP) decoders of the component codes. Differences in how the soft information is generated for the coherent and differential schemes are outlined in the next section.

3 Receiver Structures

At the receiver of an m -way MIMO-OFDM system, if there is no Doppler spread and the channel spread is shorter than the cyclic prefix, the matched filtered output at the i^{th} receive element for the k^{th} subcarrier can be written as,

$$Y_k^i = [\mathbf{X}_k^1 \mathbf{X}_k^2 \dots \mathbf{X}_k^m] [\mathbf{H}_k^{i1} \mathbf{H}_k^{i2} \dots \mathbf{H}_k^{im}]^T + \eta_k^i, \quad (1)$$

where X_k^u is the transmitted signal from the u^{th} element at the k^{th} subcarrier, H_k^{iu} is the channel frequency response from the u^{th} transmit to the i^{th} receive element. η_k^i are the additive Gaussian noise terms independent across receive elements and subbands.

3.1 Synchronization

Pilot symbols are commonly used to obtain synchronization information. As in the European Digital Audio Broadcast (DAB) standard, we periodically interrupt the OFDM blocks to insert chirp signals to be used for coarse synchronization. Since these signals increase overhead, we use them sparingly, inserting them only at multiple OFDM block intervals. Chirp signals are Doppler-tolerant, so they are particularly useful in channels with potentially high Doppler spreads such as UWA channels.

After this coarse pilot-based synchronization, we perform a finer-scale synchronization by auto-correlating the OFDM symbol to identify the interval formed by both copies of the cyclic prefix. That is, we take advantage of the fact that the cyclic prefix is just a copy of the tail end of the OFDM word, and is spaced at a known interval. This provides the basis for a maximum likelihood (ML) estimator of the timing offset as described in [11]

$$\Lambda_{ML}(\theta) = \underset{\theta}{\operatorname{argmax}} \sum_{n=\theta}^{\theta+N_g-1} (R\{y_n^* y_{n+N}\}) - \frac{\xi}{2} \{|y_n|^2 + |y_{n+N}|^2\}, \quad (2)$$

where θ is the estimate of the starting point of the OFDM frame, y_n is the sample of the received signal at time n , $\xi = \frac{E_x}{E_x + N_0}$, $\frac{N_0}{2}$ is the noise variance, E_x is the energy of the symbol, and N_g is the length of the cyclic extension. At high SNRs, the ML estimator approximates the square difference estimator since ξ approaches 1, whereas at low SNRs the estimator approximates the correlation estimator since ξ approaches 0.

A carrier frequency offset (CFO) due to the mismatch between receiver and transmitter clocks or due to Doppler may degrade the orthogonality of the subcarriers. The ML estimate of the CFO $\hat{\epsilon}$ is given by [12],

$$\hat{\epsilon} = \frac{1}{2\pi} \operatorname{argmax}_{\theta} \operatorname{arg} \left(\sum_{n=\theta}^{\theta+N_g-1} y_n y_{n+N}^* \right). \quad (3)$$

In MIMO systems, timing and frequency offsets must be estimated for each receive element.

3.2 Coherent Receiver

In OFDM, since each subcarrier experiences a flat fading channel, the channel at each subcarrier can be represented by a complex scalar multiplicative factor, which greatly simplifies channel estimation. For example, in a 2-transmitter system, the equation for the channel factors (one for each of the two transmitters) at the first receive element is:

$$\begin{pmatrix} Y_k^1 \\ Y_{k+1}^1 \end{pmatrix} = \begin{pmatrix} X_k^1 & X_k^2 \\ X_{k+1}^1 & X_{k+1}^2 \end{pmatrix} \begin{pmatrix} H_k^{11} \\ H_k^{12} \end{pmatrix} + \begin{pmatrix} \eta_k^1 \\ \eta_k^2 \end{pmatrix}. \quad (4)$$

where we have used the assumption that the k^{th} and $(k+1)^{\text{th}}$ subcarriers see exactly the same channel fades. In matrix form, this becomes

$$\hat{\mathbf{Y}}_k = \mathbf{X}_k \mathbf{H}_k + \boldsymbol{\eta}_k, \quad (5)$$

Then the least squares (LS) estimate of the channel coefficients becomes [13],

$$\hat{\mathbf{H}}_{ls} = (\mathbf{X}_k^H \mathbf{X}_k)^{-1} \mathbf{X}_k^H \hat{\mathbf{Y}}_k. \quad (6)$$

The channel estimates obtained at periodically spaced pilot tones are interpolated to provide a channel estimate at all of the subcarriers. Although this is not optimal, it has produced adequate results in our data. Finally, we note that the same approach can be used for more than two transmit elements with only minor modifications.

Once the channel is estimated for all subcarriers, we employ MAP decoding (which is the optimal approach) to detect the transmitted bits. That is, for each transmitted bit c_k , we calculate

$$\text{LLR}(c_k) = \log \frac{\text{P}(c_k = 1 | \mathbf{Y})}{\text{P}(c_k = 0 | \mathbf{Y})} = \log \frac{\sum_{X_j | c_k = 1} \text{P}(X_j | \mathbf{Y})}{\sum_{X_j | c_k = 0} \text{P}(X_j | \mathbf{Y})}, \quad (7)$$

where \mathbf{Y} denotes the received signal, and X_j is the set of symbols simultaneously transmitted from multiple elements (formed by multiple bits). Using Bayes'

rule, assuming that the transmitted symbols are equally likely and the noise variances are identical at different receivers (denoted by $\frac{N_0}{2}$), we can write

$$\text{LLR}(c_k) = \log \frac{\sum_{X_j | c_k = 1} \exp \left(-\frac{(\|\mathbf{Y} - X_j \mathbf{H}\|)^2}{N_0} \right)}{\sum_{X_j | c_k = 0} \exp \left(-\frac{(\|\mathbf{Y} - X_j \mathbf{H}\|)^2}{N_0} \right)}, \quad (8)$$

which can further be approximated as

$$\text{LLR}(c_k) \approx \frac{1}{N_0} \left(\min_{x_j | c_k = 1} \|\mathbf{Y} - X_j \mathbf{H}\|^2 - \min_{x_j | c_k = 0} \|\mathbf{Y} - X_j \mathbf{H}\|^2 \right). \quad (9)$$

For an uncoded system, these LLR values are passed to a detection device. For the turbo coded case, they are input to the iterative turbo decoder.

Finally, we note that zero forcing or MMSE detection algorithms can be used instead of the MAP detector described above to simplify the implementation [13].

3.3 Differential Receiver

We now describe the differential detectors used for single-transmitter and MIMO transmission schemes. The main difference in these schemes is that they do not need the channel estimates, and exploit the fact that adjacent frequencies undergo almost identical fades. Using a single transmit element, at the receiver, the information symbols are estimated using $\hat{u}_k = y_k \cdot y_{k-1}^*$, where $*$ denotes the complex conjugation operation.

For the differential MIMO-OFDM case, assuming that there is no time variation, and the cyclic prefix used is larger than the delay spread of the channel, the matched filtered outputs at the receiver can be written as

$$\mathbf{Y}_k = \mathbf{H}_k \mathbf{X}_k + \boldsymbol{\eta}_k, \quad (10)$$

where \mathbf{Y}_k is a matrix of $n \times t$ complex values that correspond to the received signal across all n receivers for the transmitted matrix \mathbf{X}_k . The matrix \mathbf{H} is given by

$$\mathbf{H}_k = \begin{pmatrix} H_k^{11} & H_k^{12} & \dots & H_k^{1m} \\ H_k^{21} & H_k^{22} & \dots & H_k^{2m} \\ \vdots & \vdots & \ddots & \vdots \\ H_k^{n1} & H_k^{n2} & \dots & H_k^{nm} \end{pmatrix}, \quad (11)$$

where H_k^{ij} is the channel coefficient of the channel from j^{th} transmitter to the i^{th} receiver for the k^{th} subcarrier. $\boldsymbol{\eta}_k$ is the noise matrix of size $n \times t$ containing zero mean unit variance complex Gaussian independent and identically distributed (i.i.d.) random variables. The ML rule for deciding on the transmitted matrix " \mathbf{G}_k " is given by [14]

$$\hat{\mathbf{G}}_k = \operatorname{argmax}_{\mathbf{G} \in \mathcal{G}} \operatorname{ReTr}\{\mathbf{G} \mathbf{Y}_k^H \mathbf{Y}_{k-1}\}, \quad (12)$$

assuming Rayleigh fading, where $\operatorname{ReTr}(\cdot)$ denotes the real part of the trace of a matrix. Therefore, an estimate of the information sequence can easily be found from the one-to-one mapping between \mathbf{G}_k and the information bits. Since the UWA channel is not necessarily a Rayleigh fading channel, this may only be a sub-optimal approach for our case.

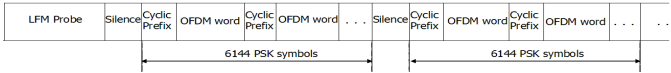


Figure 1: A frame of data.

Table 1: Uncoded (raw) data rates in the AUVfest 2007 for different schemes.

Coherent MIMO-OFDM (m=2)				
	$N=128$	$N=256$	$N=512$	$N=1024$
<i>QPSK</i>	32kbps	42.6kbps	51.2kbps	56.9kbps
8- <i>PSK</i>	48kbps	64kbps	76.8kbps	85.35kbps
Differential SISO-OFDM (m=1)				
<i>QPSK</i>	16kbps	21.3kbps	25.6kbps	28.44kbps
8- <i>PSK</i>	24kbps	32kbps	38.4kbps	42.67kbps
Differential MIMO-OFDM (m=2)				
<i>QPSK</i>	12kbps	16kbps	19.2kbps	21.3kbps
8- <i>PSK</i>	16kbps	21.3kbps	25.6kbps	28.4kbps

As in the coherent decoding, we can derive soft LLR values for the transmitted bits to be used for turbo decoding in a straightforward manner. To see this, let us define $\mathbf{Z}_k \triangleq [\mathbf{Y}_{k-1} : \mathbf{Y}_k]$. Then, for a transmitted matrix “ \mathbf{G} ”, the log likelihood ratio of the first bit is computed as

$$LLR(c_1) = \log \left(\frac{P(c_1 = 1 | \mathbf{Z}_k)}{P(c_1 = 0 | \mathbf{Z}_k)} \right), \quad (13)$$

$$= \frac{\sum_{G:c_1=1} \exp\{ReTr(\mathbf{G}\mathbf{Y}_k^H \mathbf{Y}_{k-1})\}}{\sum_{G:c_1=0} \exp\{ReTr(\mathbf{G}\mathbf{Y}_k^H \mathbf{Y}_{k-1})\}}, \quad (14)$$

where the sequence of P bits $\{c_1, \dots, c_P\}$ uniquely choose a code matrix \mathbf{G} . The computation of the LLRs for all the bits can be performed in a similar manner.

4 Experimental Results

In order to test this general MIMO-OFDM framework for UWA communications, we have participated in the AUVfest 2007 experiment off the coast of Panama City, Florida, in June 2007. For this experiment, a transmission bandwidth of 16 kHz centered at 34 kHz is used with varying number of subcarriers (128, 256, 512 and 1024), with BPSK, QPSK and 8 PSK constellations. A cyclic prefix of 8 ms is used to eliminate the effects of ISI, and different packets are separated by silent intervals of duration 100 ms. The structure of the transmitted data frames is illustrated in Figure 1. A linear frequency modulated probe signal precedes each transmission. The OFDM word (or packet) length is determined by the number of subcarriers used. Turbo codes having rates of 3/4 or 1/2 with $(5/7)_{octal}$ generators are used for an outer channel code. The interleaver lengths are 4608 or 3072 resulting in codewords of 6144 bits.

The uncoded data rates are shown in Table 1. The reported rates span a wide range up to 85 kbps obtained with the two transmit elements and 8-PSK modulation. For the coherent MIMO-OFDM, these rates need to be multiplied by $\frac{3}{4}$ to account for the pilot symbols. With turbo coding the results should also be multiplied by the code rate to find the actual transmission rate.

Tables 2 and 3 show the decoding results for coherent MIMO-OFDM transmission for different ranges. The

Table 2: Coherent uncoded MIMO-OFDM results at a horizontal distance of 500m.

	Uncoded symbol error rates			
	$N=128$	$N=256$	$N=512$	$N=1024$
<i>QPSK</i> _{2x2}	0.3737	0.2963	0.2913	0.1941
<i>QPSK</i> _{2x4}	0.3008	0.2007	0.2064	0.0898
<i>QPSK</i> _{2x8}	0.2412	0.1467	0.1334	0.0334
8- <i>PSK</i> _{2x2}	0.4097	0.3919	0.3610	0.2713
8- <i>PSK</i> _{2x4}	0.3794	0.3650	0.2824	0.1931
8- <i>PSK</i> _{2x8}	0.3251	0.3075	0.2219	0.1335

Table 3: Coherent uncoded MIMO-OFDM results at a horizontal distance of 2500m.

	Uncoded symbol error rates			
	$N=128$	$N=256$	$N=512$	$N=1024$
<i>QPSK</i> _{2x2}	0.2797	0.2396	0.1328	0.0719
<i>QPSK</i> _{2x4}	0.2196	0.1598	0.0838	0.0204
<i>QPSK</i> _{2x8}	0.1073	0.0392	0.0184	0.0017
8- <i>PSK</i> _{2x2}	0.3079	0.2735	0.2024	0.1332
8- <i>PSK</i> _{2x4}	0.2641	0.2190	0.1233	0.0681
8- <i>PSK</i> _{2x8}	0.1909	0.1430	0.0883	0.0348

Table 4: Single transmitter differential OFDM results, with a rate 3/4 outer turbo code.

	Uncoded symbol error rates			
	$N=128$	$N=256$	$N=512$	$N=1024$
<i>QPSK</i>	0.08822	0.00374	0.0013	0.00114
8- <i>PSK</i>	0.4847	0.19108	0.03223	0.00326
Coded bit error rates				
<i>QPSK</i>	0.02365	0	0	0
8- <i>PSK</i>	0.18736	0.07465	0	0

Table 5: Differential MIMO-OFDM results with a rate 1/2 outer turbo code.

	Uncoded symbol error rates			
	$N=128$	$N=256$	$N=512$	$N=1024$
<i>QPSK</i> _{500m}	0.37551	0.09779	0.02011	0.00271
<i>QPSK</i> _{2000m}	0.02597	0.00586	0.00220	0.00071
8- <i>PSK</i> _{500m}	0.38884	0.20152	0.07611	0.01650
8- <i>PSK</i> _{2000m}	0.09446	0.02807	0.01021	0.00586
Coded bit error rates				
<i>QPSK</i> _{500m}	0.39063	0	0	0
<i>QPSK</i> _{2000m}	0	0	0	0
8- <i>PSK</i> _{500m}	0.39779	0.23047	0	0
8- <i>PSK</i> _{2000m}	0	0	0	0

Table 6: Differential MIMO-OFDM results with a rate 3/4 outer turbo code.

	Uncoded symbol error rates			
	$N=128$	$N=256$	$N=512$	$N=1024$
<i>QPSK</i> _{1000m}	0.09819	0.05284	0.01067	0.00413
8- <i>PSK</i> _{1000m}	0.13632	0.10423	0.05499	0.01916
<i>QPSK</i> _{1500m}	0.03289	0.00847	0.00163	0.00065
8- <i>PSK</i> _{1500m}	0.13078	0.04544	0.02085	0.00581
Coded bit error rates				
<i>QPSK</i> _{1000m}	0.10406	0.03168	0	0
8- <i>PSK</i> _{1000m}	0.15169	0.1101	0.02886	0
<i>QPSK</i> _{1500m}	0.00716	0	0	0
8- <i>PSK</i> _{1500m}	0.1697	0.02431	0.00014	0

subscript after QPSK and 8-PSK in the first column denotes the number of transmit and receive elements used. Incorporating the outer turbo code significantly reduced the error rates. For example, all errors were eliminated in the QPSK case at a range of 500 m, with $N = 1024$, $R_c = 1/2$, and 8 receive elements. This was also observed at the 2.5 km range using a code rate of $R_c = 3/4$ and 4 or 8 receive elements. The respective transmission rates for these two cases (also taking into account the loss due to the pilot tones) are 21.3 kbps and 32 kbps.

Table 4 presents the error rates obtained with single transmitter differential OFDM at a range of 2500 m, when the conventional differential detection with turbo decoding is used. Tables 5 and 6 show the results of differential MIMO-OFDM transmission with two transmit elements. For the QPSK case, the group code was described earlier, and for the 8-PSK case the group code with 16 elements developed in [14] is employed. The results are obtained by averaging over two transmissions in the QPSK cases and three transmissions in the 8-PSK cases.

To summarize, it is observed that QPSK performs better than 8-PSK due to the larger separation between the constellation points. This gain in performance with QPSK comes at a tradeoff with the data rate. Also, higher error rates are seen when the transmitter-receiver distance is 500 m. This is due to the larger multipath delay spread of the channel at 500 m. The other visible trend here is that the error rate decreases with the number of subcarriers " N ". This is due to the fact that increasing the number of sub-carriers in a given bandwidth reduces the sub-carrier spacing. Hence, for coherent detection, the channel estimates improve with large N (assuming the same pilot overhead). Similarly for differential detection, the assumption of highly correlated fades across adjacent sub-carriers become more accurate, leading to performance improvement. The disadvantage with having a large N , however, is the increased sensitivity to Doppler shifts and Doppler spreads.

5 Conclusions

In this paper, we have described OFDM systems using both single and multiple transmitters in shallow water UWA channels, using both coherent and differential detection. We have presented results of testing our systems during a recent experiment (AUVfest 2007). These results demonstrate that high data rates with low error probabilities can be consistently achieved at a variety of ranges using OFDM and turbo codes.

Acknowledgments

This experiment was made possible through funding from the ONR SignalEx and PLUSNet programs (Tom Curtin), an ONR-funded STTR project (Bob Headrick), and an ONR-funded MURI project on acoustic communications (Bob Headrick). We gratefully acknowledge our experiment collaborators: V. Keyko McDonald and Andy Huizinga of SPAWAR Systems Center San Diego and Lee Freitag and Keenan Ball of Woods Hole Oceanographic

Institution who provided the transmit and receive arrays, respectively, and were instrumental in conducting the sea tests at AUVfest. From HLS Research, Katherine Kim organized the experiment and served as chief scientist.

References

- [1] M. Stojanovic, J. A. Catipovic and J. G. Proakis, "Phase-coherent digital communications for underwater acoustic channels," *IEEE J. Oceanic Eng.*, vol. 19, no. 1, pp. 100–111, Jan 1994.
- [2] A. Glavieux and S. Cotelan "Design and test of a coded OFDM system on the shallow water acoustic channel," *IEEE Oceans'94*, vol. 3, no. 1, pp. 472–477, Sept. 1994.
- [3] W. K. Lam and R. F. Ormondroyd, "A coherent COFDM modulation system for a time-varying, frequency selective underwater acoustic channel," *IEEE International Conference on Electronic Engineering in Oceanography*, pp. 198–203, June 1997.
- [4] M. Stojanovic, "Low Complexity OFDM detector for underwater acoustic channel," in *Proc. of MTS/IEEE OCEANS Conference*, Boston, MA, pp. 18–21, Sept. 2006.
- [5] M. Chitre, S.H. Ong and J. Potter, "Performance of coded OFDM in very shallow water channels and snapping shrimp noise," *Proceedings of MTS/IEEE OCEANS*, vol. 2, pp. 996–1001, 2005.
- [6] B. Li, S. Zhou, M. Stojanovic, L. Freitag and P. Willet, "Multicarrier communication over underwater acoustic channels with nonuniform Doppler shift," *IEEE Journal of Oceanic Engineering*, to appear 2008.
- [7] I. E. Telatar, "Capacity of a multi-antenna Gaussian channels," *European Transactions on Telecommunications*, vol. 10, pp. 585–595, Nov/Dec 1999.
- [8] V. Tarokh, N. Seshadri, and A. R. Calderbank, "Space-Time Codes for High Data Rate Wireless Communication: Performance Criterion and Code Construction," *IEEE Transactions on Information Theory*, vol. 44, no. 2, pp. 744–765, Mar 1998.
- [9] S. Roy, T.M. Duman, V. McDonald and J.G. Proakis, "High-Rate Communication for Underwater Acoustic Channels Using Multiple Transmitters and Space Time Coding: Receiver Structures and Experimental Results," *IEEE J. Oceanic Eng.*, vol. 32, no. 3, pp. 663–688, July 2007.
- [10] B. Li, and S. Zhou, M. Stojanovic, L. Freitag, J. Huang, and P. Willet "MIMO-OFDM over an Underwater Acoustic Channel," *Proc. of MTS/IEEE OCEANS Conference*, Vancouver, BC, Canada, pp. 1-6, Sept. 2007.
- [11] J. J. van de Beek, M. Sandell, M. Isaksson, and P. O. Borjesson, "Low-complex frame synchronization in OFDM systems," *IEEE Int. Conf. on Universal Personal Communications*, Tokyo, Japan, pp. 982–986, Nov. 1995.
- [12] J. J. van de Beek, M. Sandell, and P. O. Borjesson, "ML estimation of time and frequency offset in OFDM systems," *IEEE Trans. Signal Processing* vol. 45, no. 7, pp. 1800–1805, July 1997.
- [13] T.M. Duman and A. Ghayeb, *Coding for MIMO Communication Systems*, Wiley, 2008.
- [14] B. L. Hughes, "Differential Space-Time Modulation," *IEEE Transactions on Information Theory*, vol. 46, no. 7, pp. 2567–2578, Nov. 2000.